THE JOURNAL OF COMPARATIVE NEUROLOGY 472:395–410 (2004)

# Tectal Mosaic: Organization of the Descending Tectal Projections in Comparison to the Ascending Tectofugal Pathway in the Pigeon

**BURKHARD HELLMANN, ONUR GÜNTÜRKÜN, AND MARTINA MANNS***
Abteilung Biopsychologie, Institut für Kognitive Neurowissenschaft, Fakultät für Psychologie, Ruhr-Universität Bochum, 44780 Bochum, Germany

ABSTRACT

The optic tectum of vertebrates is an essential relay station for visuomotor behavior and is characterized by a set of connections that comprises topographically ordered input from the eyes and an output that reaches premotor hindbrain regions. In the avian tectofugal system, different ascending cell classes have recently been identified based on their dendritic and axonal projection patterns, although comparable information about the descending cells is missing. By means of retrograde tracing, the present study describes the detailed morphology of tectal output neurons that constitute the descending tectobulbar and tectopontine pathways in pigeons. Descending cells were more numerous in the dorsal tectum and differed in terms of 1) their relative amount of ipsi- vs. contralateral projections, 2) the location of the efferent cell bodies within different tectal layers, and 3) their differential access to visual input via dendritic ramifications within the outer retinorecipient laminae. Thus, the descending tectal system is constituted by different cell classes presumably processing diverse aspects of the visual environment in a visual field-dependent manner. We demonstrate, based on a careful morphological analysis and on double-labeling experiments, that the descending pathways are largely separated from the ascending projections even when they arise from the same layers. These data support the concept that the tectum is arranged as a mosaic of multiple cell types with diverse input functions at the same location of the tectal map. Such an arrangement would enable the tectal projections onto diverse areas to be both retinotopically organized and functionally specific. J. Comp. Neurol. 472:395–410, 2004.


**Indexing terms: tectum opticum; superior colliculus; tectobulbar pathway; tectopontine pathway; extrageniculocortical pathway; birds**

In vertebrates, the optic tectum is an essential relay station for visuomotor transformation. In accordance with this function, the tectum is characterized by an evolutionally conserved set of projections conveying ascending visual output to the forebrain and descending projections to premotor hindbrain regions. Despite this similar assembly of efferent neurons, the size and laminar organization of the tectum vary considerably among vertebrate species (Reiner, 1994).

Two distinct tectal pathways convey visual information to the forebrain in amniotes. One of them arises from neurons characterized by wide dendritic fields projecting to the nucleus rotundus in sauropsids (Karten et al., 1997; Luksch et al., 1998; Hellmann and Güntürkün, 2001; Dávila et al., 2002; Belekhova et al., 2003; Marín et al., 2003) or the lateral posterior/pulvinar nucleus in mammals (Major et al., 2000, and references therein). These diencephalic structures are then the source of projections

Grant sponsor: SFB Neurovision of the Deutsche Forschungsgemeinschaft; Grant sponsor: Alfried Krupp-Stiftung.

*Correspondence to: Martina Manns, Biopsychologie, Institut für Kognitive Neurowissenschaft, Fakultät für Psychologie, Ruhr-Universität Bochum, 44780 Bochum, Germany.
E-mail: martina.manns@ruhr-uni-bochum.de

Received 10 October 2003; Revised 16 December 2003; Accepted 22 December 2003

DOI 10.1002/cne.20056

Published online the week of March 29, 2004 in Wiley InterScience (www.interscience.wiley.com).

to diverse telencephalic structures (sauropsids: Benowitz and Karten, 1976; Nixdorf and Bischof, 1982; Guirado et al., 2000; Laverghetta and Shimizu, 2003; mammals: Lin and Kaas, 1980; Beck and Kaas, 1998). A second tectal efferent system arises from radial neurons with small-field dendrites projecting to the dorsolateral thalamus, from which projections lead to the forebrain (Gamlin and Cohen, 1986; Wild, 1989; Harting et al., 1991; Martinez-Marcos et al., 1998; Belekhova et al., 2003). In amphibians, similar cell types innervate dorsal and ventral thalamic areas (Lazar et al., 1983; Dicke and Roth, 1996; Dicke, 1999; Roth et al., 1999). Descending tectal information is conveyed by ipsi- and contralateral projections to premotor hindbrain regions. In amniotes, an ipsilateral tectopontine pathway (ITP) can be distinguished from a crossed tectobulbar pathway (CTB; or predorsal bundle in mammals; for review see Reiner, 1994). Comparably to the ascending projections, the descending pathways are constituted of radial and multipolar cell populations. The similarity of ascending and descending efferent cell types in tetrapodes is considered as important evidence for the common origin of these cells (Reiner, 1994). The morphological and electrophysiological similarities of the characteristic wide-field neurons in birds and mammals are so striking that Major et al. (2000) termed this a "cellular homology."

Despite these cellular similarities between tetrapods, the ascending and descending efferent systems display considerable cytoarchitectonic variations concerning the laminar localization of their cell bodies, their axonal projection patterns, and their dendritic lamination and, hence, their access to retinal input. In amphibians, ascending and descending cells are intermingled, and single cells eventually give rise to axons with collaterals projecting to both thalamus and hindbrain (Dicke, 1999; Roth et al., 1999). In amniotes, ascending and descending cells migrate during development to a differential degree into the superficial laminae (Reiner, 1994). In the mammalian superior colliculus, most tectal neurons with descending projections lie deeper than those with ascending projections (for review see Reiner, 1994). In contrast, sauropsids display a substantial overlap in the localization of ascending and descending cell bodies, although morphological data suggest that both populations represent separate cells types (Reiner and Karten, 1982; Reiner, 1994; Karten et al., 1997). A detailed analysis of ascending and descending tectal cell types in sauropsids is partly hampered by the insufficient definition of "superficial" and "deep" with respect to the location of cells along the tectal z-axis. Although the stratum opticum of the mammalian superior colliculus provides a clear means to discriminate cells in the stratum griseum superficiale with monosynaptic retinal input as "superficial" and those with indirect polysynaptic retinal input in the stratum griseum intermedium and below as nonretinorecipient and "deep," such a simple differentiation is not feasible in sauropsids. In birds, for example, the majority of cells in the deep layer 13 should in fact be classified as "superficial" because of their dendritic ramifications within the superficial retinorecipient layers (Karten et al., 1997) and their monosynaptic retinal input (Hardy et al., 1984). Subpopulations of efferent tectal cells display unique dendritic arborization patterns within distinct tectal laminae and are innervated by different retinal ganglion cells types (mammals: Harrell et al., 1982; Ogawa et al., 1985; Abramson and Chalupa, 1988; Mooney et al., 1988a; Major et al., 2000; birds: Karten et al., 1990; Hellmann and Güntürkün, 1999, 2001; Luksch et al., 2001). Thus, they probably process qualitatively divergent visual information. These functionally divergent ascending tectal cell types converge in different thalamic substructures, so a transformation from a retinotopic to a functionotopic organization is required (Wang et al., 1993; Hellmann and Güntürkün, 2001; Marín et al., 2003). Neurophysiological studies suggest comparably separate descending channels from the tectum to premotor hindbrain areas that encode distinct parameters of stimulus location (Masino and Grobstein, 1989; Masino and Knudsen, 1990). However, the subserving tectal cell types are not well characterized, and it is unclear how the retinotopic coding of the tectum is transformed into visuomotor coordinates.

Birds display the highest degree of tectal differentiation, with at least 15 distinguishable laminae (according to Cajal, 1911). Neurons ascending to the dorsal and ventral thalamus (Gamlin and Cohen, 1986; Wild, 1989) and a subpopulation of neurons descending within the tectopontine tract arise from cells whose somata are located within intermediate layers 8–10 (Reiner and Karten, 1982). Cells establishing projections to the rotundus and a large portion of cells descending into the brain stem are located in efferent layer 13 (Benowitz and Karten, 1976; Reiner and Karten, 1982; Hellmann and Güntürkün, 2001). Recently, the neuronal elements of the ascending tectorotundal pathway, which connects the tectum via the diencephalic nucleus rotundus with the telencephalic ectostriatum, have been studied in detail. These cells are differentiated into at least five subtypes, demonstrating the high degree of complexity of the tectorotundal system (Karten et al., 1997; Luksch et al., 1998; Hellmann and Güntürkün, 2001; Marín et al., 2003). This constitutes an excellent basis for comparative description of the descending neuronal elements. The clarification of how far the ascending information is separated from the descending information in such a highly differentiated visual system as the avian tectofugal pathway might help to elucidate the functional organization principles of tectal visuomotor processing.

The present work, based on a detailed morphological comparison of ascending and descending neuronal populations as well as on double-labeling experiments, demonstrates that both pathways emerge from largely separated tectal cell groups. Additionally, our study suggests that, similarly to the ascending tectal projections, the descending tectal efferents also constitute a mosaic of diverse cell types that transform a retinotopic code into segregated functional domains.

## MATERIALS AND METHODS

Seventeen adult pigeons (*Columba livia*) of both sexes from local breeding stocks were used in this study. To identify the localization of the descending cell populations, choleratoxin subunit B (CtB; Sigma, Deisenhofen, Germany) was injected unilaterally either into the lateral tegmentum to label the tectopontine fiber tract (n = 5; Fig. 1A) or into the medial tegmentum to label the tectobulbar fiber tracts (n = 8; Fig. 1B) at rostrocaudal levels A1.25–A3.00 (Karten and Hodos, 1967). Additionally, two animals received bilateral injections of CtB into the rostromedial mesencephalic tegmentum at the level of nucleus

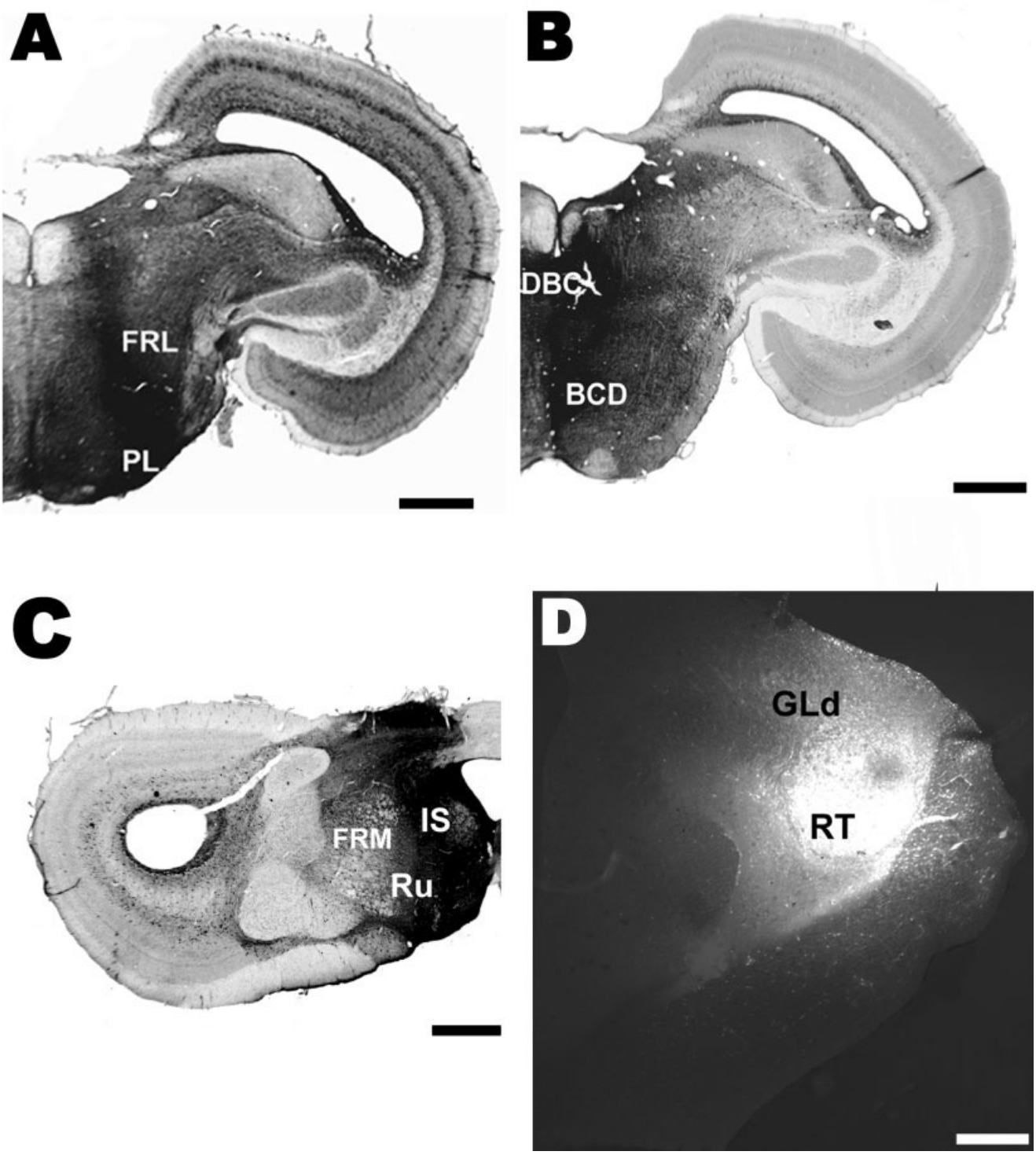


Fig. 1. Photomicrographs of tracer injection sites. **A:** To label the tectopontine system (ITP), tracer injections were placed in the lateral tegmental region of the FRL. **B:** To label the tectobulbar system (CTB), tracers were applied to the medial tegmental region of BCD and DBC. Note that the PL as the target of the ITP was not labeled, indicating the specificity of the medial injection. **C:** To label tectal efferents projecting to the rostral tegmentum, tracer was injected into the rostromedial tegmentum, including Ru/IS. **D:** To label the ascending tectal cell populations, TDA was injected into the RT and GLd. BCD, brachium conjunctivum descendens; DBC, decussatio brachiorum conjunctivorum; FRL, formation reticularis lateralis mesencephali; FRM, formation reticularis medialis mesencephali; GLd, nucleus geniculatus lateralis, pars dorsalis; IS, nucleus interstitialis (Cajal); PL, nucleus pontis lateralis; RT, nucleus rotundus; Ru, nucleus ruber. Scale bars = 1,000 μm in A–C, 500 μm in D.

ruber and nucleus interstitialis (Cajal; Fig. 1C). All CtB-injected animals also received bilateral injections of Texas red dextran amine (TDA; 10,000 MW, lysine fixable; Molecular Probes, Leiden, The Netherlands) into the central and dorsal diencephalon (Fig. 1D). All experiments were carried out according to the specifications of the German law for the prevention of cruelty to animals.

Prior to surgery, the pigeons were anesthetized with equithesin (0.31–0.33 ml/100 g body weight), and the animals were placed into a stereotaxic apparatus (Karten and Hodos, 1967). The scalps were infiltrated with xylocaine and incised dorsally. Next, the skull was opened with a dental drill, and a glass micropipette (outer tip diameter 20 μm) mounted to a mechanic pressure device (WPI nanoliterinjector) was inserted into varying sites of the brain (diencephalic injections: anterior 5.3–7.0, dorsal 5.0–8.5, lateral 1.8–3.8; rostromedial tegmentum: anterior 3.5–4.5, dorsal 5.0–7.0, lateral 0.5–0.9; lateral tegmentum: anterior 1.5–2.5, dorsal 3.0–4.0, lateral –1, with 15° dorsolateral slant; medial tegmentum: anterior 1.5–2.5, dorsal 2.0–4.0, lateral 0.5) according to the stereotaxic coordinates of the pigeon brain atlas by Karten and Hodos (1967). Injection depths ranged from 1.0 to 2.8 mm. In cases of tegmental injections, approximately 50 nl CtB [1% (w/v) in distilled water] were injected in steps of 2 nl over a period of 15–20 minutes. Diencephalic injections were performed with 100 nl TDA [10% (w/v) in 2% dimethyl sulfoxide]. Subsequently, the pipette was removed, and the skin was infiltrated again with xylocaine and sutured.

After 2 days of survival, animals received an injection of 200 U sodium heparin and were then deeply anesthetized with an overdose of equithesin (0.55 ml/100 g body weight). The pigeons were perfused through the heart with 100 ml 0.9% (w/v) sodium chloride and 800 ml ice-cold 4% paraformaldehyde in 0.12 M phosphate buffer (PB), pH 7.4. The brains were removed and stored for 2 hours in fixative with a supplement of 15% sucrose (w/v). Subsequently, the brains were stored overnight in a solution of 30% sucrose in 0.12 M PB. On the following day, the brains were cut in the frontal plane at 35 μm on a freezing microtome, and the slices were collected in PB containing 0.1% sodium azide (w/v).

Brain slices were reacted freely floating according to the immuno-ABC technique. The sections were placed for 35 minutes in 0.5% hydrogen peroxidase in distilled water to reduce endogenous peroxidase activity. In cases of sole CtB detection, sections were incubated overnight at 4°C in the primary antibody [rabbit anticholeragenoid; Sigma Germany; 1/20,000 in 0.12 M PB with the addition of 2% NaCl (w/v), 0.3% Triton X-100 (v/v), and 5% normal goat serum]. After being rinsed, the sections were incubated for 60 minutes at room temperature in the biotinylated secondary antibody (goat anti-rabbit; Vectastain; Vector Camon, Wiesbaden, Germany; 1/250 in 0.12 M PB + 2% NaCl + 0.3% Triton X-100). After additional rinsing, the sections were incubated for 60 minutes in avidin-biotin-peroxidase solution (Vectastain ABC-Elite Kit, Vector Camon; 1/100 in 0.12 M PB + 2% NaCl + 0.3% Triton X-100). After washing, the peroxidase activity was detected by using a heavy-metal-intensified 3′3-diaminobenzidine (DAB; Sigma) reaction (Adams, 1981), modified by the use of β-d-glucose/glucose oxidase (Sigma) instead of hydrogen peroxidase (Shu et al., 1988). The sections were mounted on gelatin-coated slides, dehydrated, and coverslipped with Permount (Fisher Scientific, Fair Lawn, NJ). Some sections were counterstained with cresyl violet. In one series of sections (every tenth section), primary CtB antibody was detected with a secondary fluorescein-labeled antibody (goat anti-rabbit; Vector), which was incubated for 1 hour at room temperature (1/75 in 0.12 M PB + 2% NaCl + 0.3% Triton X-100). Subsequently, sections were rinsed, mounted on gelatinized slides, and coverslipped with the ProLong Antifade Kit (Molecular Probes, Eugene, OR). Sections were observed with an Olympus BH2 epifluorescence microscope with the following filter settings: for fluorescein, Olympus IB set with additional shortpass emission filter G520; for TDA, Chroma filters (Brattleboro, VT) with excitation filter HQ-577/10, dichroic mirror Q-585LP, and emission filter HQ-645/75.

The rotundal tracer injection sites and the resulting retrograde CtB labeling within the optic tectum were analyzed with an Olympus BH2 microscope. Qualitative reconstructions of the rotundal/triangular CtB diffusion area and of the position of labeled somata as well as their peripheral processes were made in Nissl-counterstained sections. Drawings were made using digitized microscopic images (JVC-TK C1381 and GrabitPCI grabber; SIS, Münster, Germany) in the PC software Designer 3.1 (Micrografx). Quantitative determinations of soma size, number, and distribution of the labeled cells were performed on digitized images with the help of an image-analysis system (analySIS 3.0 Doku; SIS). Statistical analysis was performed with the help of the PC-based statistical program Statistica (StatSoft, Tulsa, OK).

The number of retrogradely labeled layer 13 somata was estimated within the ipsilateral as well as contralateral tectum along a rostrocaudal extent of 2.8 mm (A1.5–A4.3; Karten and Hodos, 1967) by counting fluorescein-labeled CtB-filled cells in every tenth section at ×450 magnification. The amount of fluorescein/TDA double-labeled cells was determined by manual marking fluorescein-labeled cells in digital images and by a projection of these marks onto the corresponding digital image with Texas red label. We were interested only in an estimation of the number of double-labeled cells relative to the number of cells with sole fluorescein label. Therefore, no correction procedures were used. Photographic documentation was carried out with a digital camera system (Zeiss Axiocam) attached to the microscope. Images were processed with Zeiss Axiovision 3.0 and Photoshop 5.5 software. Color balance, contrast, and brightness were adjusted to a variable extent to achieve satisfying output results with the Fuji "Media-Lab" printer device.

## RESULTS

### Tectopontine system

CtB injections into the lateral tegmentum (n = 5; Fig. 1A) labeling the tectopontine pathway resulted in tracer spread along rostrocaudal levels between A1.50 and A3.75. Overall, the number of labeled cells, counted in every tenth section, varied between 249 and 3,387 (mean 1,788, SD 1,389). Despite these large quantitative differences, the tectal labeling pattern was very similar in all cases and differed substantially from the pattern of medial tegmental injections. Retrogradely labeled neurons were located primarily within the ipsilateral tectum, with

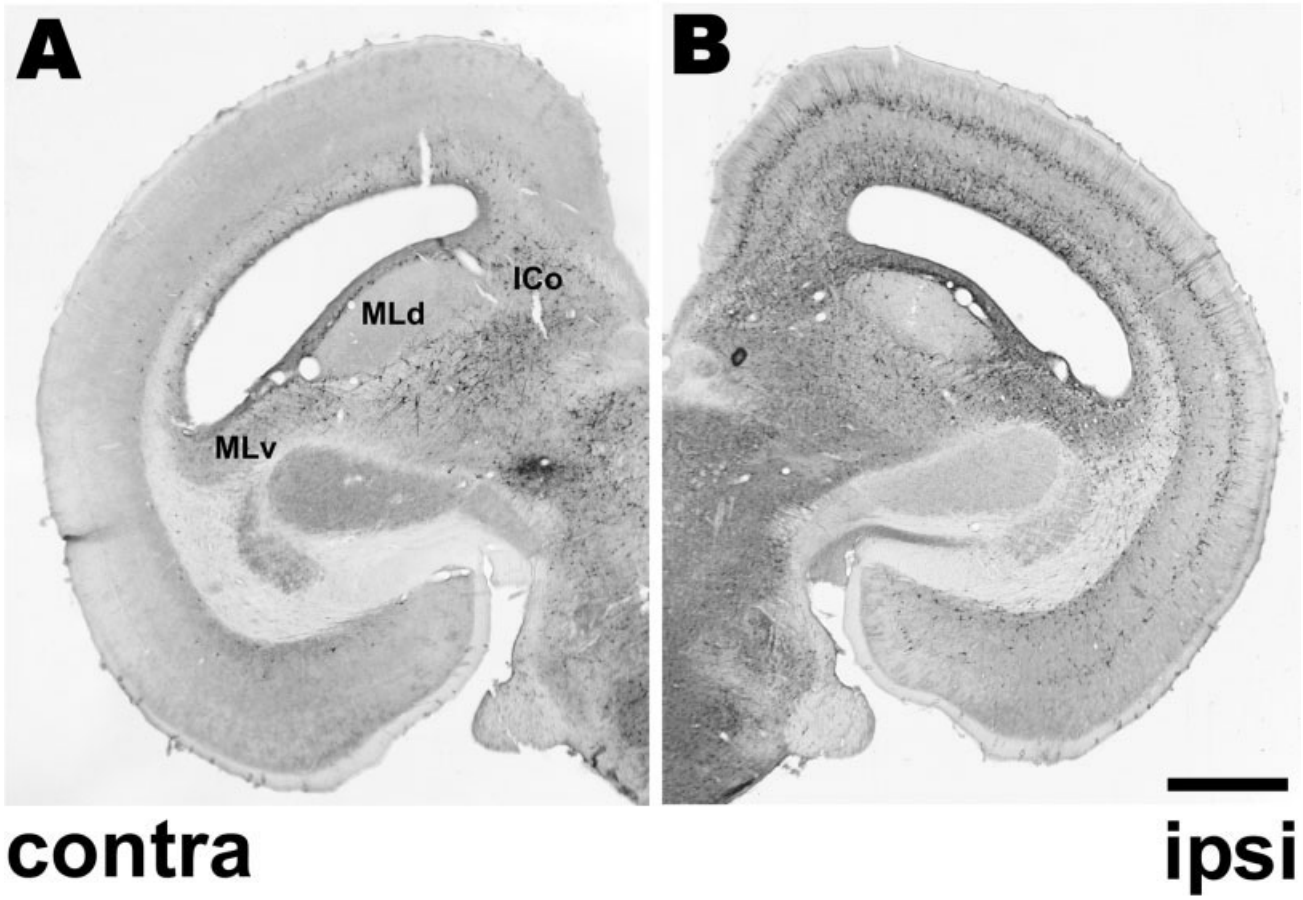


Fig. 2. Photomicrographs of both tectal hemispheres after CtB injections into the right lateral tegmentum, labeling the tectopontine pathway (ITP). The ipsilateral tectum (**A**) contained the majority of labeled cells roughly clustered within an inner and an outer row of neurons. Within the contralateral tectum (**B**), labeled cells were confined to deep layers 12 and 13. Ico, nucleus intercollicularis; MLd, nucleus mesencephalis lateralis, pars dorsalis; MLv, nucleus mesencephalis lateralis, pars ventralis. Scale bar = 1,000 μm.

a mean of 77% (SD 22.75%) of all labeled cells located on the ipsilateral side. Within the ipsilateral tectum, cell bodies formed two rows. The outer row consisted of cells located within layers 6–10 (Figs. 2, 3B). Most of their somata were located within the outer part of layer 10. Most of these cells, located exclusively within the ipsilateral tectum (Fig. 3), exhibited neurites of probably dendritic nature, which entered the outer retinorecipient laminae and bifurcated extensively within layers 2–5a (Fig. 4). Many superficial layer 10 cells as well as most cells located within layers 6–9 exhibited a single or two main dendrites, which were directed toward the outer retinorecipient layers. Ramification widths of single radial dendrites ranged between 50 and 100 μm within layers 3–4. In the case of two radially oriented processes, interdendrite distances within layer 5b were between 20 and 100 μm (Fig. 4B). Radial cells also exhibited smaller dendrites that originated at the medial or lateral soma and took a lateral to medial course. These processes could be followed to tectal layers 9–11. In contrast to radial cells, somata located in central to deep layer 10 often exhibited thick horizontal dendrites, which could be followed for up to 300 μm in lateral extent. Horizontal layer 10 dendrites irregularly gave rise to radial processes that could be followed to retinorecipient layer 3 (Fig. 4B).

Although only few labeled cells were visible in layers 11 and 12, high numbers of layer 13 neurons were labeled (Figs. 2, 3). These multipolar cells were located throughout peripheral to deep sublayers. Horizontally oriented dendritic ramifications of these cells could be followed for up to 500 μm within layer 13. High densities of CtB-filled processes were also present in layer 12. Within layer 11, only few, thin fibers could be detected, and these processes could often be identified as dendritic ramifications of layer 10 cells, suggesting that dendritic processes of multipolar layer 13 cells rarely reached higher than tectal layer 12. Within the dorsal tectum, a considerable number of multipolar cells also extended into layer 14. From these large (up to 55 μm diameter), fusiform to round cells, dendritic processes were directed in both horizontal and radial directions (Fig. 5). Smaller cells with ovoid somata (diameter around 20 μm) were also labeled in periventricular tectal layer 15. Both layer 14 and layer 15 cells were restricted to tectal regions that overlaid the tectal ventricle. In the ventrolateral tectum, the inner band of tectal somata was restricted to layer 13 cells. Dorsally, layer 14

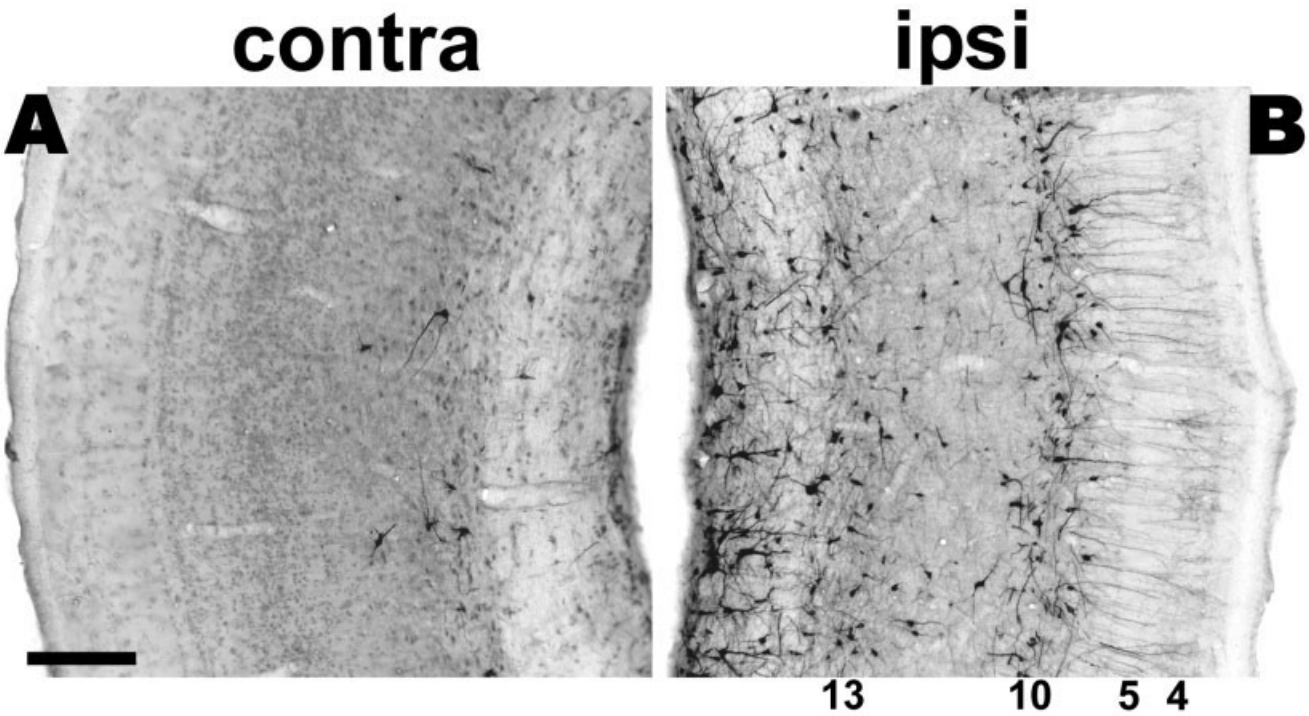


Fig. 3. Photomicrographs of the contralateral (**A**) and ipsilateral (**B**) tectum after labeling of the tectopontine pathway. Within the ipsilateral tectum, cells of the outer row (layers 7–10) frequently exhibited dendrites ascending into the outer retinorecipient layers. In contrast, processes of neurons located in deeper layers 12–15 did not reach higher than layer 11. This was also apparent for all neurons located in the contralateral tectum. Scale bar = 200 μm.

and 15 cells passed over into the nucleus intercollicularis, whereas, ventrally, cells contributed to nucleus mesencephalis lateralis, pars ventralis (Fig. 2).

A minority of labeled cells (22.9%, SD 22.7) was located within the contralateral tectum (Figs. 2, 3A). The labeling pattern differed from that of the ipsilateral side, in that all cell bodies were confined to layers 12–15. Cells exhibited the same features (distribution, shape, extent) as neurons within the inner row of the ipsilateral tectum (Fig. 3A,B). Possibly because of the fact that an outer row of cells was missing, labeled processes were absent superficially to layer 11. In the ipsilateral as well as in the contralateral tectum, the number of back-filled somata was highest in the dorsal one-third of the optic tectum and lowest within the ventral segment (Friedman ANOVA: df 8.00, $P < .05$; Fig. 6A).

## Tectobulbar system

CtB injections into the ventromedial tegmentum (n = 8; Fig. 1B) labeling the tectobulbar pathway resulted in tracer spread along rostrocaudal levels between A1.75 and A4.00. The tectobulbar fibers crossed within the decussatio brachiorum conjunctivorum (DBC; Fig. 1B), but virtually no fibers could be detected descending within the contralateral tegmentum, supporting the specificity of our medial injections. The number of labeled cells, counted in every tenth section, varied between 300 and 5,818 (mean 2,317, SD 2,559). Although the amount of retrogradely filled cells exhibited considerable variation, the resulting qualitative labeling pattern did not. Medial tegmental injections labeled cells in deep tectal layers 12–15 within both hemispheres. An outer row of cells, as labeled after lateral tegmental CtB injections, was virtually absent. In contrast to the case with lateral tegmental injections, the contralateral tectum contained the majority of labeled cells, with a mean of 59.4% (SD 22.7%) of all labeled cells located on the contralateral side; Fig. 7). Within the ventral tectum, most cells were present within layer 13 (Figs. 7, 8). Additionally, few cells were labeled in layer 12. These cells exhibited the same morphological features as layer 13 cells, with multipolar fusiform to round somata (diameter 22.8 μm, SD 6.0). Processes of labeled somata often ramified in horizontal to lateral directions. These presumably dendritic processes could be followed for up to 350 μm in lateral/horizontal directions, and they typically did not ascend more superficially than to tectal layer 11 (Fig. 8A,C). Only five cells were detected to exhibit thick radial processes reaching into tectal layer 2 (Fig. 9). Somata located in layer 12 exhibited roughly the same morphological features as layer 13 neurons and may, therefore, be regarded as displaced layer 13 cells. Within layer 14, labeled cells of both hemispheres were often smaller (19.9 μm diameter, SD 9.4) and showed stronger morphological variation, with multipolar round to extremely fusiform shapes with the long axis oriented both radially and horizontally (Fig. 8D). Additionally, few cells were labeled in periventricular layer 15. As with lateral tegmental CtB injections, the number of retrogradely labeled somata was highest in the dorsal one-third, significantly decreasing from the dorsal to ventral one-thirds of the ipsi- as well as the contralateral tectum (Friedman ANOVA: df 9.750, $P < .01$; Fig. 6B).

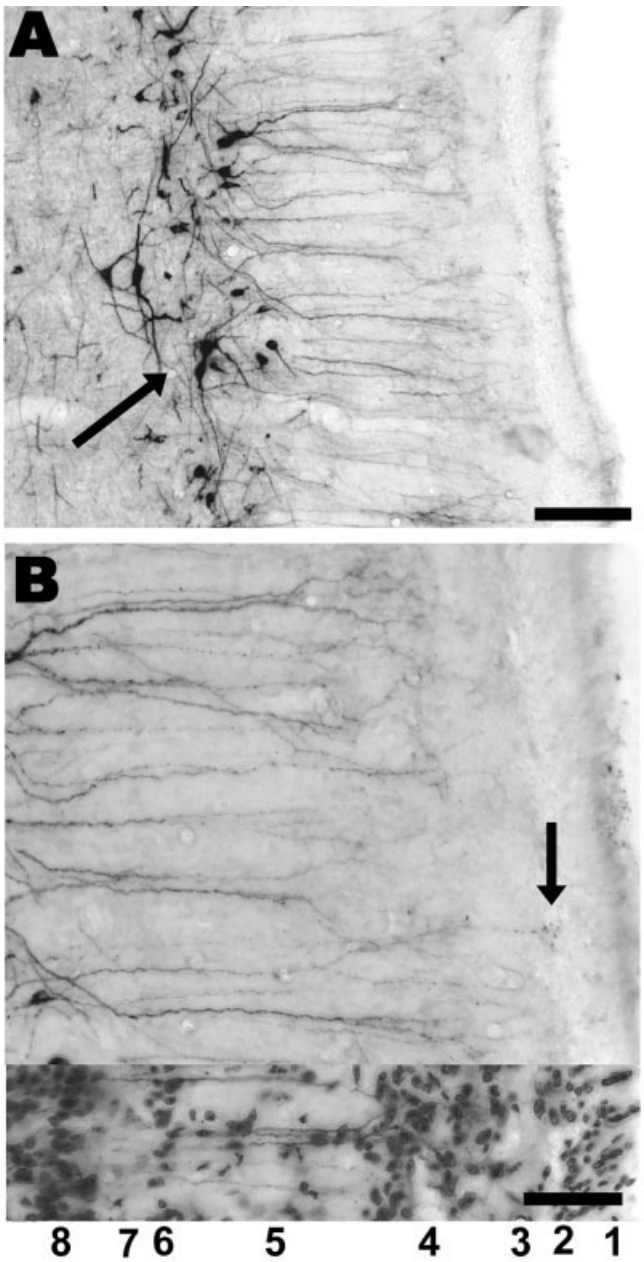


Fig. 4. Higher magnification of cells labeled after lateral tegmental CtB injections labeling the tectopontine pathway. **A:** CtB filled cells of the outer row located in layers 8–10. Whereas the more superficially situated neurons often formed radial processes, primary dendrites of cells located in layer 10 were often horizontally oriented. Secondary, radially to tangentially oriented ramifications were observed to arise from these horizontal arbors (arrow). **B:** Higher magnification of the outer tectal layers. Dendritic ramifications with probably postsynaptic swellings were located in layers 4 and 3 (arrow). A corresponding, cresyl violet-counterstained section is attached to allow better visualization of tectal lamination (bottom numbers). Scale bars = 100 μm in A, 50 μm in B.

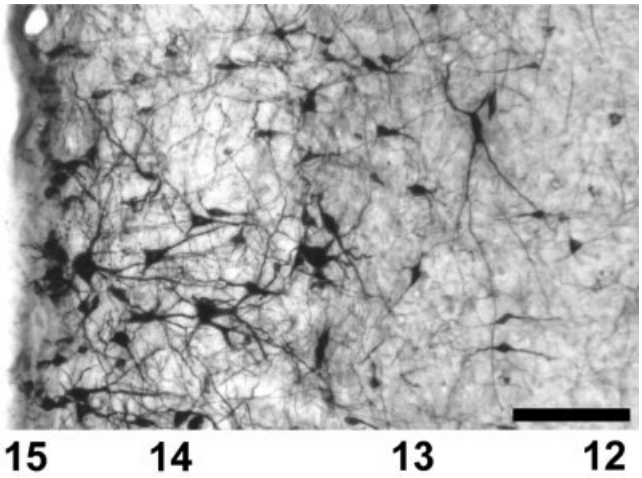


Fig. 5. Higher magnification of layers 12–15 of the ipsilateral tectum after lateral tegmental CtB injections labeling the tectopontine system. Scale bar = 100 μm.

In two animals, injections into the rostromedial tegmentum at the level of the nucleus ruber and nucleus interstitialis (Cajal) were performed (Figs. 1C, 10). Both injections labeled high numbers of tectal cells (1,497 and 2,097 somata counted in every tenth section). In both animals, neurons were only faintly labeled; the CtB reaction product was limited to the cell bodies and thick proximal processes. As with more caudally situated medial tegmental injections, the overwhelming majority of cells was located in inner tectal layers 12–15. Compared with ventromedial tracer injections, two major variations were observed: 1) Most CtB filled cells were located in the ipsilateral (88.8% and 93.2%) and not the contralateral hemisphere and 2) in the lateral and especially the ventral tectum, minor numbers of cell bodies (5.9% and 9.1% of all neurons) were also filled in layer 10 or 11. No labeling was observed in the outer retinorecipient layers. However, because of the poor intensity of the labeling, we cannot exclude dendritic ramifications within these layers. In fact, the fusiform and radially oriented shape of some layer 10/11 cell bodies points to this possibility. As in all other cases, cells of inner layers 14 and 15 were nearly restricted to the dorsal tectum, with these cell bands located in a periventricular position and passed over to nuclei intercollicularis and mesencephalis lateralis, pars ventralis.

## Double-labeling experiments

To examine whether tectal output neurons contribute to both the ascending and the descending tectofugal pathways, a second fluorescent tracer (TDA) was injected into the central thalamus to label the nucleus rotundus (Fig. 1D). In nearly all animals, TDA labeled bilaterally high numbers of tectal cells within tectal layer 13 (Fig. 11). Additionally, in some cases, a band of cells within deep tectal layer 10 was filled within the ipsilateral tectum. These cells exhibited radial processes that typically extended to the superficial retinorecipient laminae. Insofar as labeling of these cells was always associated with substantial TDA spread into the dorsal thalamus, these cells presumably represent the ascending output that innervates the nucleus geniculatus lateralis, pars dorsalis (GLd; Wild, 1989).

In all animals that exhibited substantial labeling of both the ascending (TDA) and the descending (CtB) tectal

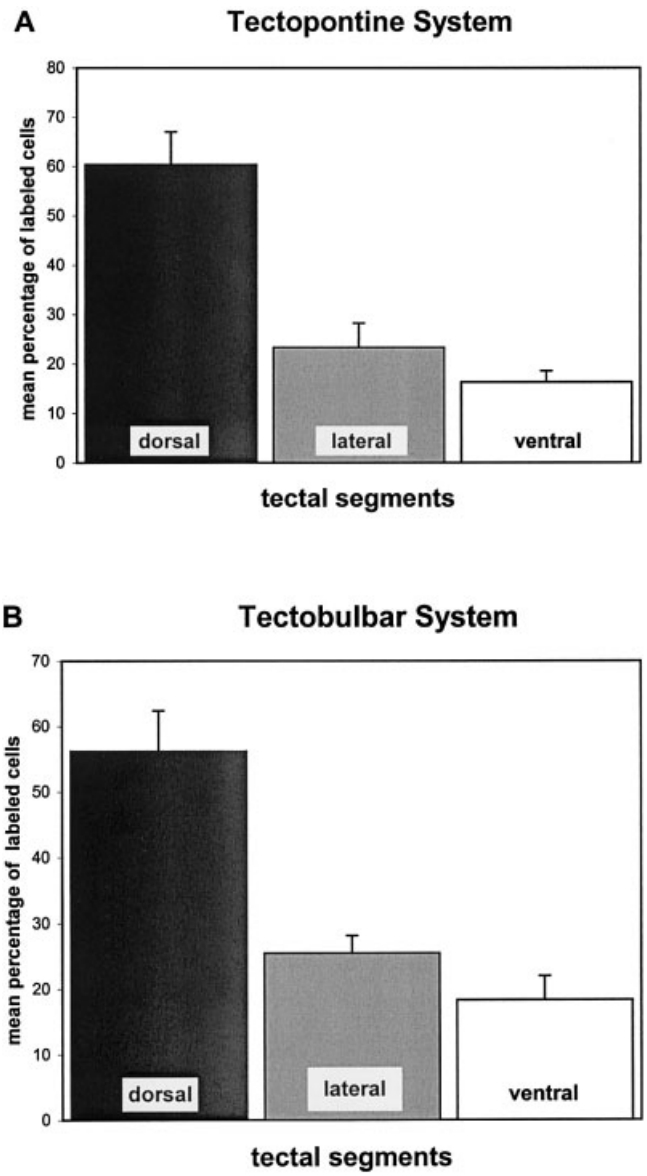


Fig. 6. Mean percentage of retrogradely labeled cells in the dorsal, lateral, and ventral tectal segments after lateral (**A**) or medial (**B**) tegmental CtB injections. In both experimental groups, the proportion of labeled cells differed significantly between tectal segments. The frontal plane of the tectal sections was subdivided into three segments according to Manns and Güntürkün (1997).

projections, the amount of double-labeled cells was determined. After all tegmental injections, the proportion of double-labeled cells (relative to the number of CtB-filled cells) was extremely low, 0.38% (n = 7, SD 0.55) for medial tegmental and 0.26% (n = 4, SD 0.12) for lateral tegmental injections. The only animal with a rostral tegmental CtB injection combined with thalamic TDA injections exhibited 0.33% double-labeled cells. Thus, the data strongly suggest that the tectal cell populations that contribute to the ascending thalamic and descending tegmental projections are nearly completely segregated, although the cell bodies are located at least to some degree in the same tectal layers.

## DISCUSSION

The present paper describes the detailed morphology of tectal output neurons that establish the descending contralateral tectobulbar (CTB) and the ipsilateral tectopontine (ITP) pathways in pigeons. These systems differ in terms of 1) their relative amounts of ipsilateral vs. contralateral projections, 2) the location of the efferent cell bodies within different tectal layers, and 3) their differential access to visual input via dendritic ramifications within the outer retinorecipient tectal layers. Despite an overlap in the laminar location with ascending cells, double labeling showed a virtually complete separation of ascending and descending projection neurons.

The use of the highly sensitive tracer choleratoxin demonstrated a higher portion of bilateral projections than had been previously demonstrated (Karten and Revzin, 1966; Reiner and Karten, 1982) and revealed a detailed picture of the axonal and dendritic branching pattern. This allows us to compare the morphology of descending cells with that of the well-described ascending neurons (Karten et al., 1997; Luksch et al., 1998; Hellmann and Güntürkün, 2001). In principle, two main groups of descending tectal efferents can be distinguished based on the laminar localization of their cell bodies. Whereas the tectopontine pathway emerges from two cellular populations located within layers 6–12 and layers 13–15, the tectobulbar tract arises virtually exclusively from layers 13–15. According to the dendritic arborization pattern, the two descending pathways receive variable visual input, which differs from the input conveyed to ascending cells. The differential access to retinal input points to the processing of different aspects of the visual environment and hence corresponds to the differential role in visuomotor behavior. Studies in a wide range of species suggest that the crossed tectobulbar tract is involved in approach and orientation toward a novel, desired object, whereas the ipsilateral tectopontine pathway participates in movements away from obstacles or aversive stimuli (Ingle, 1983; Dean et al., 1988; Ellard and Goodale, 1988). As outlined in detail below, the cells of the descending systems are not overlapping with those constituting other tectal projection streams.

### The layer 6–10 system

After lateral tegmental CtB injections labeling the tectopontine pathway, an outer band of cells was detected, which combines somata located within ipsilateral layers 6–10. Only in these cases was a labeling of distal cell processes within retinorecipient layers 2–5a detected. Most of these processes could be directly verified as dendrites of pyramidal cells of layers 8–10 or multipolar cells within layers 9 and 10. Based on the extent of their dendritic ramifications over the tectal surface, these two groups could be distinguished as “widefield” multipolar layer 10 cells vs. “narrowfield” pyramidal layer 8–10 cells. Individual ramifications of the “widefield” neurons typically could be followed for up to 300 μm in the lateral direction. This dendritic pattern is comparable to that of ascending multipolar “type I” layer 13 neurons labeled after CtB injections into the rotundus (Karten et al., 1997; Luksch et al., 1998; Hellmann and Güntürkün, 2001). However, whereas the typical bottlebrush endings of these cells arborize within layer 5b, the dendrites of descending cells tend to branch in layers 2–5a.

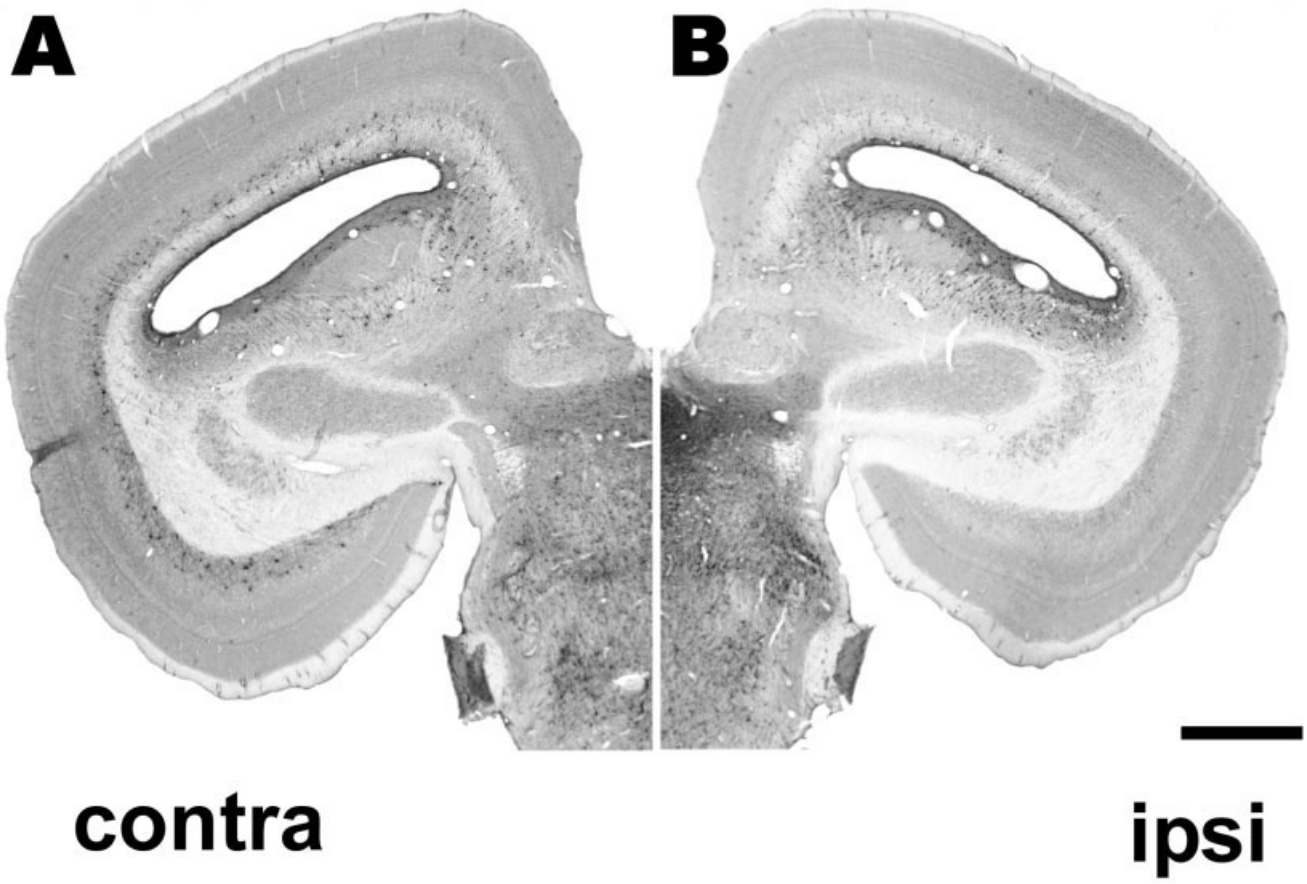


Fig. 7. Photomicrographs of the contralateral (**A**) and ipsilateral (**B**) tectal halves after CtB injections into the right ventromedial tegmentum, labeling the tectobulbar pathway (CTB). Neuronal somata were located predominantly in the contralateral hemisphere. On both sides, labeled cells were confined to deep layers 12 and 15. Scale bar = 1,000 μm.

Although the multipolar layer 10 neurons share some dendritic features of tectal neurons that establish the ascending tectorotundal pathway in layer 13, the pyramidal cells of layers 8–10 do definitely not. Instead, they display characteristics comparable to those of radial efferent neurons in layers 8–11 (Hunt and Brecha, 1984). These latter cells project onto the isthmic nuclei nucleus isthmoopticus (ION; Crossland and Hughes, 1978; Uchiyama and Watanabe, 1985; Woodson et al., 1991); nucleus isthmi, pars parvocellularis (Ipc; Hunt et al., 1977); and nucleus isthmi, pars semilunaris (SLu; Hellmann et al., 2001) and onto the thalamic nucleus geniculatus lateralis, pars ventralis (GLv; Hunt and Künzle, 1976; Crossland and Uchwat, 1979) and GLd (Gamlin and Cohen, 1986; Wild, 1989). A morphological comparison reveals that all these cells represent cell classes that differ from the descending tectopontine neurons.

Ipc-projecting neurons exhibit a single spiny apical dendrite arborizing within layers 3, 5, and 9. These cells are characterized by an axon arising from the apical process as a shepherd's crook (Hunt et al., 1977; Woodson et al., 1991). Thus, these cells differ from the near-field ITP-projecting cells displaying dendritic arborizations in layers 2–5a.

In contrast, the apical dendritic arborizations and the location of the somata at the border between layers 9 and 10 suggest a good match between ITP- and ION-projecting cells (Uchiyama and Watanabe, 1985; Woodson et al., 1991; Uchiyama et al., 1996). However, because the ION-projecting cells do not possess ascending dendrites extending into superficial layers 2–7 and because ITP near-field neurons lack the extensive basal dendritic ramifications within tectal layers 12–14, which are typical for ION afferents (Uchiyama et al., 1996), ITP- and ION-projecting neurons probably likewise represent different cell populations.

As with the ITP-projecting cells, GLd afferents were shown to be located primarily within layers 6–10 of the dorsal tectum (Gamlin and Cohen, 1986; Wild, 1989). Our rotundal TDA injections often resulted in considerable tracer spread within the dorsally located GLd and hence retrogradely labeled its tectal input. Compared with the ITP-projecting cells, these radial neurons were located slightly more at the outer surface of layer 10. Additionally, double labeling of ascending and descending projections revealed virtually no double-labeled cells. Thus, we can definitely exclude a common origin for tectal ITP and GLd afferents. Comparable assertions regarding whether GLv and ITP projections result from axon collaterals of a com-

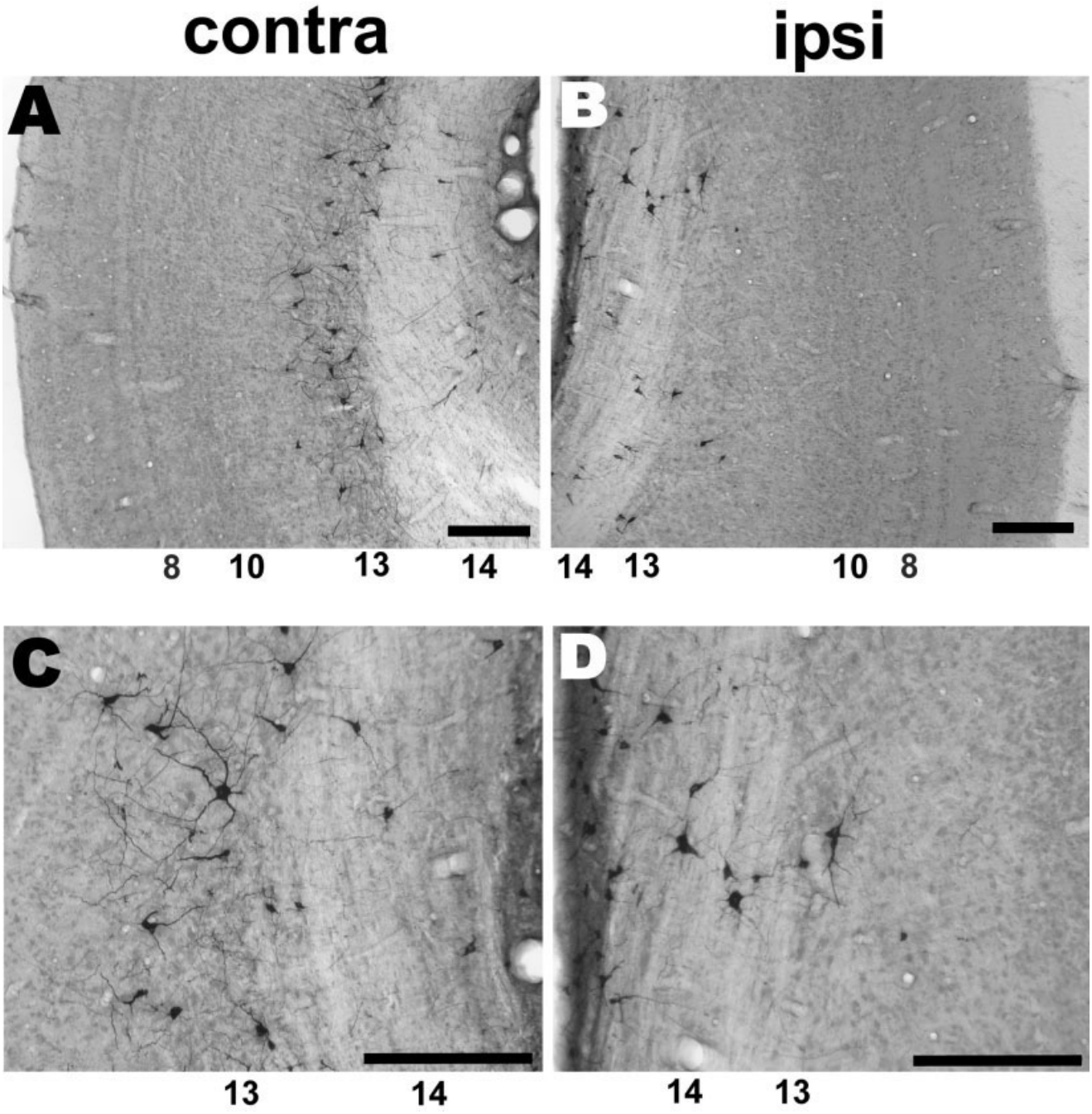


Fig. 8. Higher magnification of retrogradely labeled cells after medial tegmental injections labeling the tectobulbar pathway: **A** and **B** depict all ipsi- and contralateral tectal layers. **C** and **D** show labeled cells in deep tectal layers 12–15 in more detail. On both sides, dendritic processes of the multipolar neurons were restricted to layers 12–14. Scale bars = 200 μm.

mon pool of tectal near-field neurons were not possible with our experiments.

Our results present a picture of a highly differentiated system of tectal efferents within the intermediate layers: Although tectal projections onto GLv, GLd, IPC, ION, and the ITP system all arise from the same tectal layer, each target region seems to be innervated by a unique set of layer 10 neurons. This is further supported by a multiple sublayering of this major source of tectal output detected by means of different calcium-binding proteins (unpublished data).

## The layer 13–15 system

Our results revealed a substantial number of tegmentally descending cells to be located in the deep tectal

layers 13–15. Cells located in layer 13 were intermingled with neurons constituting the exclusive source of tectorotundal projection, which is the major ascending visual processing stream in birds (Benowitz and Karten, 1976; Karten et al., 1997; Deng and Rogers, 1998; Hellmann and Güntürkün, 1999, 2001). Tectorotundal and descending cell populations exhibit a considerable difference in their dendritic ramification patterns. After tegmental CtB injections, ascending dendritic processes did not reach higher than up to layer 12. This is different from the labeling pattern of most ascending layer 13 neurons. These cells are differentiated into at least five subtypes characterized by dendritic arborizations within different tectal laminae (Hellmann and Güntürkün, 2001) and by projection to functionally specified subregions of the nucleus rotundus (Wang and Frost, 1992; Wang et al., 1993; Laverghetta and Shimizu, 1999; Hellmann and Güntürkün, 1999, 2001). The overwhelming majority of rotundal projecting neurons has direct access to retinal input, with dendrites reaching up to retinorecipient layers 3–5. However, one of the ascending neurons (type II) displays dendrites that do not ramify within the retinorecipient layers. Insofar as the dendrites of the descending layer 13 cells are comparably confined to the deep layers, the eventual presence of bidirectionally projecting cells could be limited to these type II cells. Type II cells constitute only a minor portion of the ascending tectofugal system and terminate in the nucleus triangularis, a dorsomedial extension of the rotundus (Karten et al., 1997; Hellmann and Güntürkün, 2001). However, our double-labeling data show that neither of the two descending systems overlaps in important numbers with ascending type II cells. The deep tectal layers 14/15 also contribute substantially to both descending pathways. These multipolar cells share dendritic features with layer 13 neurons but tend to have smaller somata. However, these cells are restricted to the dorsal tectum medially, passing over into the nucleus intercollicularis. Because their dendrites do not ascend higher than to layer 12, neither population receives direct retinal input, suggesting that they convey indirect visual and/or multimodal information. It is not known whether these cells represent a functionally specialized subtype of the descending cell population different from layer 13 neurons. Within the deep layers 14 and 15, ascending tectorotundal cells are virtually absent (Hellmann and Güntürkün, 2001). Thus, the deepest layers constitute

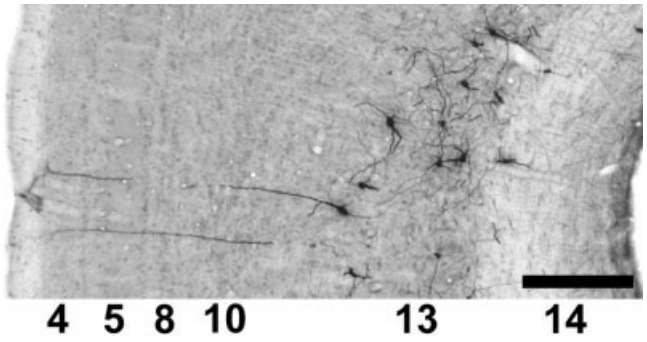


Fig. 9. After medial tegmental CtB injections labeling the tectobulbar pathway, neurons with thick radial processes directed to the outer tectal layers 2–4 were only rarely labeled. Scale bar = 200 μm.

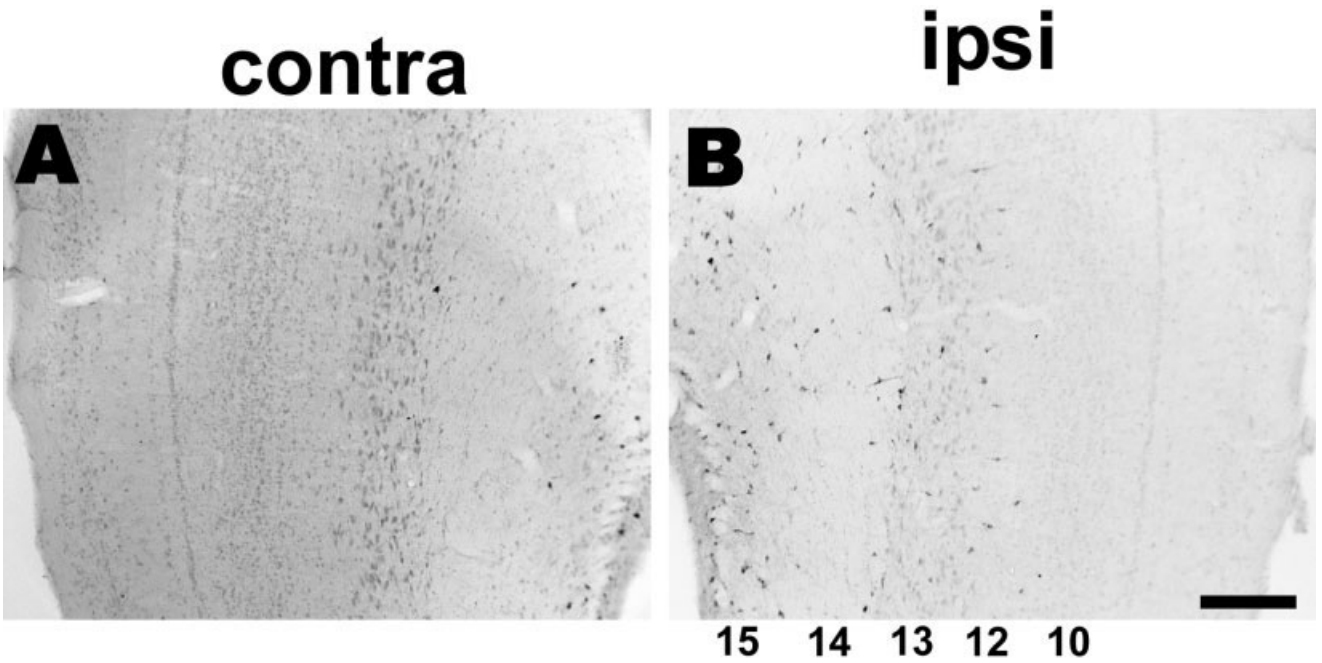


Fig. 10. Photomicrographs through all layers of the lateral contralateral (**A**) and ipsilateral (**B**) tectum after CtB injections into the rostromedial mesencephalic tegmentum. Most cells were located in layers 12–15 of the ipsilateral tectum; only few cell were labeled within layers 10–11 of the lateral and ventral tectum. Scale bar = 200 μm.

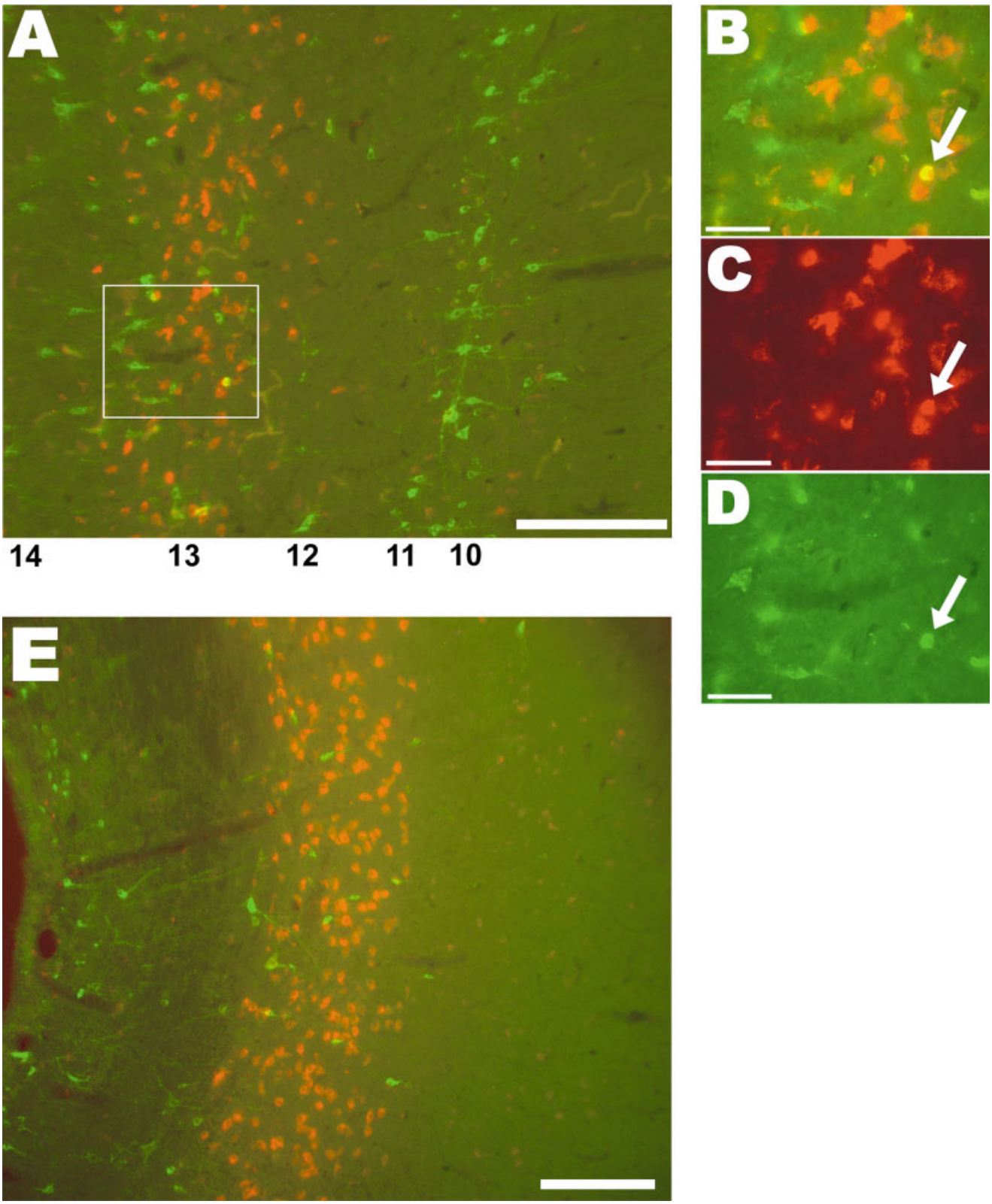


Fig. 11. **A:** Photomicrographs of layers 8–14 of the right tectum after bilateral TDA injections into the central thalamus and CtB injections into the right lateral tegmentum. Red-labeled cells are those with ascending thalamic projections, and green label indicates projections to the brainstem. Although red and green cells intermingled within deep tectal layer 13, only very few cells contained both tracers (arrows). Numbers indicate location of tectal layers. **B–D:** Higher magnification of the boxed area in A. The yellow and hence double-labeled cell in B (arrow) was visible with the Texas red (C) as well as the fluorescein (D) filter set. **E:** Photomicrograph of layers 5–15 of the right tectal hemisphere after TDA injections into the central thalamus (bilaterally) and CtB injections into the left ventromedial tegmentum. Red-labeled cells are those with ascending thalamic projections, and green-labeled cells project to the brainstem. Although red and green cells intermingled within deep tectal layer 13, no double-labeled cell could be detected. Scale bars = 200 μm in A,E, 50 μm in B–D.

purely descending projections, which is comparable to the pattern observed in other vertebrates (Reiner, 1994).

Three conclusions follow from these observations. First, the avian tectum hosts multiple descending cell types that are different from the systems giving rise to the ascending streams. Second, because of this fact, at least one further tectal layer 13 cell type with descending projections has to be added to the list of ascending tectorotundal cell types in this lamina. Third, insofar as the ascending and the descending information streams are remarkably independent from each other, they seem to constitute informationally encapsulated modules as postulated by Fodor (1983). By this line of reasoning, the multiple tectal cellular systems might operate strictly in parallel with and independent from each other as special-purpose input–output modules with prespecified functions.

## Visual field-dependent organization

The present study revealed that, apart from differences in the proportion of ipsi- and contralateral populations, the descending cells are heterogeneously distributed along the tectal dorsoventral axis. Whereas tectobulbar projections in the mallard and chick originate predominantly from the rostroventral tectum (Shepherd and Taylor, 1995; Tellegen et al., 1998), our lateral and medial tegmental tracer injections primarily labeled cells in the dorsal tectal segment. This overrepresentation of the dorsal tectum within the descending streams was clearly visible, although the ventral tectum has about twice as many neurons as the dorsal tectum (Theiss et al., 1996). This distribution is reversed from that of ascending tectorotundal cells, where, with the exception of type II, significantly more projections arise from the ventral tectum (Hellmann and Güntürkün, 1999, 2001). Because the tectum is retinotopically organized with the upper visual field represented in the dorsal and the lower and frontal visual field in the ventral tectum (Clarke and Whitteridge, 1976; Hayes et al., 1987; Remy and Güntürkün, 1991), ascending and descending tectofugal projections process information mainly from the lower and the upper visual fields, respectively. The predominance of ventral tectal projections to the rotundus can explain why rotundal lesions lead to acuity impairments only in the lower frontal field of view (Güntürkün and Hahmann, 1999). Similarly, our data suggest the descending system to be specialized to the upper visual field, represented in the dorsal tectum. The deep tectal layers receive input from the nucleus spiriformis lateralis (SpL), which conveys basal ganglia influence to the tectum and hence participates in forebrain control of the tectal premotor output (Reiner et al., 1982a). SpL is characterized by biochemical subdifferentiations (Reiner et al., 1982b), and the projection onto the tectum displays a rough dorsoventral topography (Reiner et al., 1982a; Hellmann et al., 2001), indicating a visual field-dependent modulation of premotor control. Thus, retinal information from the upper and lateral visual field seems to be preferentially analyzed with respect to premotor control, so the dorsal tectum might be specialized to allow reactions to objects emerging within this field of view.

## Segregation of ascending and descending projections

In comparing the efferent tectal cell types in tetrapods, the cells differ in 1) their receipt to retinal input, 2) the localization of the cell bodies, and 3) the degree of axonal arborizations to different targets. During evolution, a trend for the segregation of all three features seems to exist. Whereas in salamanders all efferent subtypes receive direct retinal input (Dicke, 1999; Roth et al., 1999), in amniotes the efferent cellular populations are segregated into cells receiving monosynaptic or polysynaptic retinal input. This is accompanied by a different degree to which the efferent cell bodies migrate into superficial layers during development. Although ascending and descending efferent cells are intermingled in the tectum of amphibians, these cells exhibit a high laminar separation in the mammalian superior colliculus. Different degrees of separation can be observed in sauropsids, with ascending and descending cells partially located within the same layer (Reiner, 1994; Belekhova et al., 2003). However, despite the different laminar organization patterns of the mammalian superior colliculus and the optic tectum of sauropsids, the spatial relations between the efferent projection systems are very similar. In contrast to the case for the avian tectum, retinal input enters the mammalian colliculus via the third layer from the surface, the stratum opticum. The layer superior to the stratum opticum (stratum griseum superficiale) tends to have ascending projections, although some cells located inferior to the stratum opticum also give rise to projections to several thalamic nuclei (Linke et al, 1999). Whereas neurons projecting to the GLd are located within the upper sublayers of the stratum griseum superficiale, neurons projecting to the lateral posterior/pulvinar nucleus are located within the lower stratum griseum superficiale or within the stratum opticum (for review see Reiner, 1994), whereby their ascending dendrites reach to the outermost sublayers (Major et al., 2000). Thus, this organization resembles the pattern present in the avian tectum, where GLd-projecting cells are located more superficially than tectorotundal neurons, which likewise send ascending dendrites up to the outer retinorecipient layers. Comparably to the tectopontine and tectobulbar tracts of the avian tectum, the premotor systems of the mammalian colliculus are segregated into a population descending within the tectopontine tract or within the predorsal bundle. Although most cells are located below the stratum opticum, the tectopontine tract combines two cellular populations. The ipsilaterally projecting cells are located within the stratum griseum superficiale or stratum opticum, and the contralaterally projecting neurons are localized below the stratum opticum within the deep laminae (for review see Reiner, 1994). Again, this pattern is very similar to the arrangement of the avian tectal descending system, with a superficial and a deep tectopontine population and a solely deep tectobulbar population.

It is not clear how closely the laminar segregation of tectal cells is related to a separation of axons projecting to different targets. In salamanders, single cells display axon collaterals to both ascending and descending fiber bundles (Dicke, 1999), and, in the turtle's tectum, some tectorotundal cells display side branches to the GLd (Belekhova et al., 2003). The present data show that, in pigeons, ascending and descending cells located within the same tectal layer represent completely separated cell populations. This parcellation might be related to the functional role of the tectum in visuomotor processing. Visuomotor integration might be at least in part directly obtained by efferent cells in salamanders, but, in more highly developed sys-

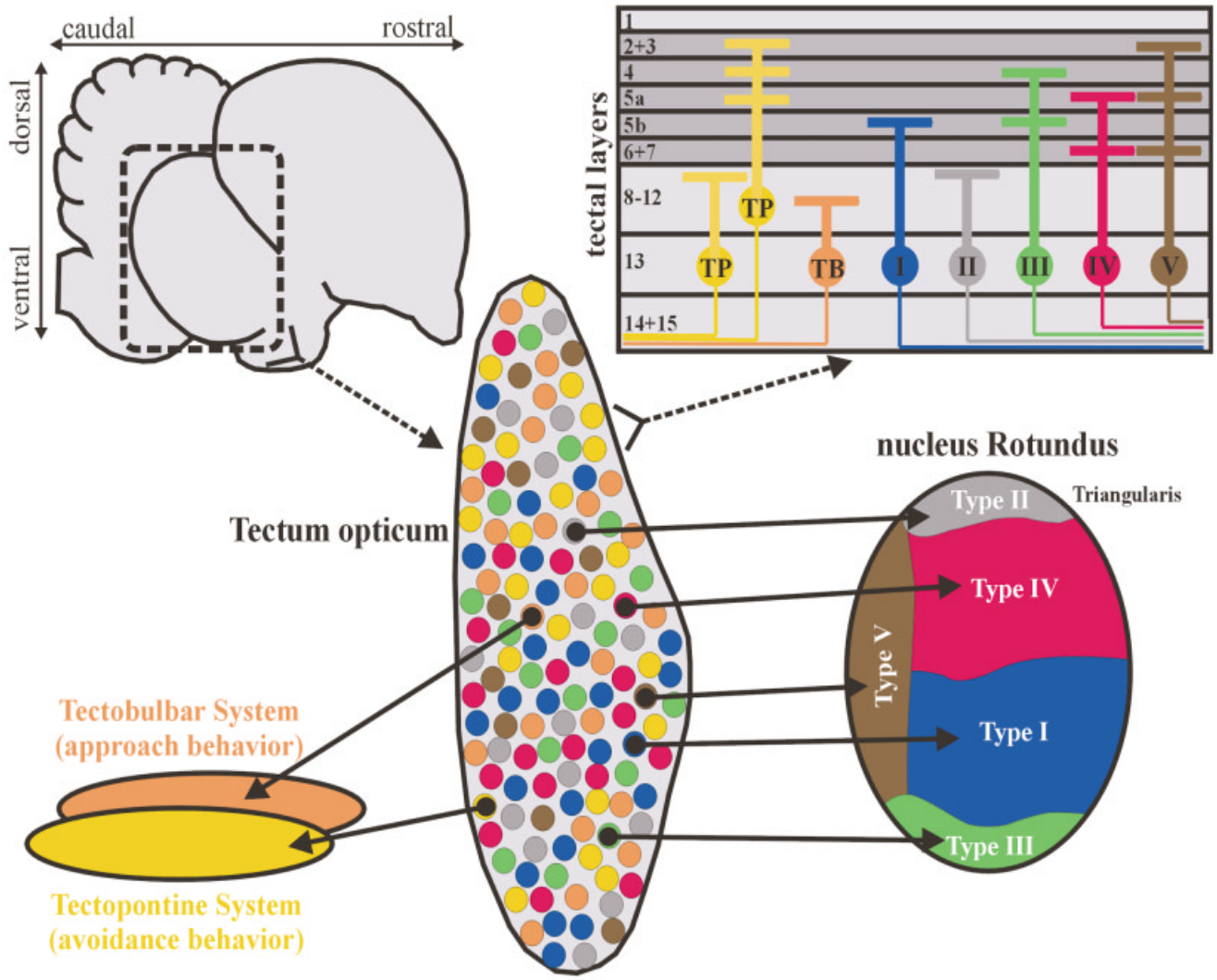


Fig. 12. Schematic outline of the tectal mosaic hypothesis. We propose that multiple cell types with diverse visual inputs at about the same location of the tectal map constitute the tectal projections onto diverse areas. These projections are both retinotopically organized and functionally specific. A pigeon brain with a highlighted optic tectum is represented at upper left. An "unfolded" tectum with a two-dimensional map of the tectal surface is shown in the center (the process of unfolding is described by Remy and Güntürkün, 1991). Small circles in different colors represent cells on the tectal map that have descending projections within the tectopontine (TP, in yellow) and the tectobulbar systems (TB, in orange) or ascending ones within the tectorotundal projection (cell types I–V). Each of these cell types projects to an area with the same color code. At upper right, a schematic cross-section of the optic tectum is shown, with retinorecipient layers 2–7 depicted in dark gray. Tectal neurons with descending projections to the brainstem and ascending projections to the rotundus are shown with their main dendritic bifurcations in the superficial tectal strata allowing a cell type-specific organization of visual input. The complete arrangement explains how functionally specific tectal projections arise from a retinotopically arranged organization.

tems, comparable functions seem to be mediated by direct or indirect contacts between sensory and motor neurons. In mammals, the transmission of visual signals from the superficial to the deep tectal layers is mediated by interlaminar connections (Mooney et al., 1988b; Isa, 2002; Doubell et al., 2003). In the avian tectum, reafferent circuits might subserve comparable functions. Apart from tectal interneurons, specialized nuclei are likely involved in such circuits. Two candidates are the nucleus isthmi pars semilunaris (SLu), a component of the isthmic complex, and the lateral spiriform nucleus (SpL). SLu has reciprocal input with the tectum and projections onto the rotundus and to the SpL (Hellmann et al., 2001). This connectivity pattern suggests that SLu plays a key role in the topographically organized modulation of the ascending projections and, indirectly, in cooperation with the SpL, also the descending projections of the tectum (Hellmann et. al., 2001). Because SpL conveys descending forebrain information to the deeper tectal layers, it is assumed to relay information regarding the bird's ongoing and impending movements in order to coordinate the bird's body position with the location of objects in the bird's visual space (Reiner et al., 1982a).

## The tectal mosaic

The present study shows that the tectum is composed of multiple cell types that constitute the diverse efferent

systems radiating from the midbrain. These efferent cell types can be distinguished from each other by several morphological criteria, such as laminar position, dendritic arrangement, and target structures. Because tectal laminae differ in their visual and nonvisual input (Miceli et al., 1987; Yamagata and Sanes, 1995; Karten et al., 1997), we assume that the cell type-specific dendritic bifurcations within only some of the tectal layers produce idiosyncratic mixtures of afferents and thus differential functional modes for each of the diverse tectal efferent systems. At the same time, each of these efferent cells is embedded into the retinotopic arrangement of the tectal surface, probably producing a retinotopic arrangement within all tectofugal systems. Thus, each point of the tectal space map hosts multiple cell types and the origin of multiple independent projections onto different diencephalic and brainstem structures subserving diverse functions. This mosaic-like architecture, schematically outlined in Figure 12, was first proposed by Hellmann and Güntürkün (2001) as a solution to the problem of how the retinotopic tectal map could be transformed into a functionotopic arrangement within the nucleus rotundus (Wang and Frost, 1992; Wang et al., 1993; Laverghetta and Shimizu, 1999). Recently, Marín et al. (2003) could verify this proposal in a further detailed analysis of the tectorotundal projection.

The present data extend this concept of the tectal mosaic. Both the tectopontine and the tectobulbar pathways are heterogeneous with respect to the cell types involved, both originate from the complete extent of the tectal surface (albeit predominantly dorsal), and both pathways give rise to terminal branches at different levels of the premotor reticular formation (Reiner and Karten, 1982; Tellegren et al., 1998). At the same time, the crossed tectobulbar tract is involved in approach and orientation toward desired objects, whereas the ipsilateral tectopontine pathway guides movements away from aversive stimuli (Ingle, 1983; Ellard and Goodale, 1988; Dean et al., 1988). Thus, the principle of a transformation from retinotopic to functionotopic coding as suggested for the tectofugal pathway could apply in exactly the same way for the descending tectal projections. It is even likely that these descending projections can be further subdivided within the same framework. For example, injections into the region of the nucleus interstitialis (Cajal) evinced labeled cells that are located only in layers 11–15. Thus, these cells intermingle with other neurons descending in the tectobulbar tract but vary from them in their predominance in the ipsilateral tectum and in their laminar location superficial to layer 13.

Taken together, our concept of the tectal mosaic posits that, by virtue of multiple cell types with diverse input functions at the same location of the tectal map, the projections of the optic tectum onto diverse areas can be both retinotopically organized and functionally specific. Insofar as this arrangement probably applies both for the ascending tectorotundal and for the descending tectomesencephalic pathways, it could represent a basic feature of the optic tectum that also defines the architecture of the other tectal efferents.

## LITERATURE CITED


Abramson BP, Chalupa LM. 1988. Multiple pathways from the superior colliculus to the extrageniculate visual thalamus of the cat. J Comp Neurol 271:397–418.

Adams JC. 1981. Heavy metal intensification of DAB-based HRP reaction product. J Histochem Cytochem 29:775.

Beck PD, Kaas JH. 1998. Thalamic connections of the dorsomedial visual area in primates. J Comp Neurol 396:381–398.

Belekhova M, Kenigfest N, Rio J-P, Repérant J, Ward R, Vesselkin N, Karamian O. 2003. Tectothalamic visual projections in turtles: their cells of origin revealed by tracing methods. J Comp Neurol 457:37–56.

Benowitz LI, Karten HJ. 1976. Organization of tectofugal visual pathway in pigeon: retrograde transport study. J Comp Neurol 167:503–520.

Cajál SR. 1911. Histologie du système nerveux de l'homme et des vertébrés. Paris: Maloine.

Clarke PG, Whitteridge D. 1976. The projection of the retina, including the "red area" on the optic tectum of the pigeon. Q J Exp Physiol 61:351–358.

Crossland WJ, Hughes CP. 1978. Observations on the afferent and efferent connections of the avian isthmo-optic nucleus. Brain Res 145:239–256.

Crossland WJ, Uchwat CJ. 1979. Topographic projections of the retina and optic tectum upon the ventral lateral geniculate nucleus in the chick. J Comp Neurol 185:87–106.

Dávila JC, Andreu MJ, Real MÁ, Puelles L, Guirado S. 2002. Mesencephalic and diencephalic afferent connections to the thalamic nucleus rotundus in the lizard *Psammodromus algirus*. Eur J Neurosci 16:267–282.

Dean P, Redgrave P, Mitchell IJ. 1988. Organization of efferent projections from superior colliculus to brainstem in rat: evidence for functional output channels. Prog Brain Res 75:27–36.

Deng C, Rogers LJ. 1998. Organization of the tectorotundal and SP/IPS-rotundal projections in the chick. J Comp Neurol 394:171–185.

Dicke U. 1999. Morphology, axonal projection pattern, and response types of tectal neurons in plethodontid salamanders. I: tracer study of projection neurons and their pathways. J Comp Neurol 404:473–488.

Dicke U, Roth G. 1996. Similarities and differences in the cytoarchitecture of the tectum of frogs and salamanders. Acta Biol Hung 47:41–59.

Doubell TP, Skaliora J, Baron J, King AJ. 2003. Functional connectivity between superficial and deeper layers of the superior colliculus: an anatomical substrate for sensorimotor integration. J Neurosci 23: 6596–6607.

Ellard CG, Goodale MA. 1988. A functional analysis of the collicular output pathways: a dissociation of deficits following lesions of the dorsal tegmental decussation and the ipsilateral collicular efferent bundle in the Mongolian gerbil. Exp Brain Res 71:307–319.

Fodor J. 1983. The modularity of mind. Cambridge, MA: MIT Press.

Gamlin PDR, Cohen DH. 1986. A second ascending visual pathway from the optic tectum to the telencephalon in the pigeon (*Columba livia*). J Comp Neurol 250:296–310.

Guirado S, Devila JC, Real MA, Medina L. 2000. Light and electron microscopic evidence for projections thalamic nucleus rotundus to targets in the basal ganglia, the dorsal ventricular ridge, and the amygdaloid complex in a lizard. J Comp Neurol 424:216–232.

Güntürkün O, Hahmann U. 1999. Functional subdivisions of the ascending visual pathways in the pigeon. Behav Brain Res 98:193–201.

Hardy O, Leresch N, Jassik-Gerschenfeld D. 1984. Postsynaptic potentials in neurons of the pigeon's optic tectum in response to afferent stimulation from the retina and other visual structures. Brain Res 311:65–74.

Harrell JV, Caldwell RB, Mize RR. 1982. The superior colliculus neurons which project to the dorsal and ventral lateral geniculate nucleus in the cat. Exp Brain Res 46:234–242.

Harting JK, Huerta MF, Hashikawa T, van Lieshout DP. 1991. Projection of the mammalian superior colliculus upon the dorsal lateral geniculate nucleus: organization of tectogeniculate pathways in nineteen species. J Comp Neurol 304:275–306.

Hayes BP, Hodos W, Holden AL, Low AL. 1987. The projection of the visual field upon the retina of the pigeon. Vis Res 27:31–40.

Hellmann B, Güntürkün O. 1999. Visual-field-specific heterogeneity within the tecto-rotundal projection of the pigeon. Eur J Neurosci 11:2635–2650.

Hellmann B, Güntürkün O. 2001. The structural organization of parallel information processing within the tectofugal visual system of the pigeon. J Comp Neurol 429:94–112.

Hellmann B, Manns M, Güntürkün O. 2001. Nucleus isthmi, pars semilunaris as a key component of the tectofugal visual system in pigeons. J Comp Neurol 436:153–166.

Hunt SP, Brecha N. 1984. The avian optic tectum: a synthesis of morphol-

ogy and biochemistry. In: Vanegans H, editor. Comparative neurology of the optic tectum. New York: Plenum Press. p 619–648.

Hunt SP, Künzle H. 1976. Observations on the projections and intrinsic organization of the pigeon optic tectum: an autoradiographic study based on anterograde and retrograde, axonal and dendritic flow. J Comp Neurol 170:153–172.

Ingle D. 1983. Brain mechanisms of visual localization by frogs and toads. In: Ewert JP, Capranica RR, Ingle D, editors. Advances in vertebrate neuroethology. New York: Plenum Press. p 177–226.

Isa T. 2002. Intrinsic processing in the mammalian superior colliculus. Curr Opin Neurobiol 12:668–677.

Karten HJ, Hodos W. 1967. A stereotaxic atlas of the brain of the pigeon. Baltimore: Johns Hopkins Press.

Karten HJ, Revzin AM. 1966. The afferent connections of the nucleus rotundus in the pigeon. Brain Res 2:368–377.

Karten HJ, Keyser KT, Brecha N. 1990. Biochemical and morphological heterogeneity of retinal ganglion cells. In: Cohen B, Bodis-Wollner I, editors. Vision and the brain. New York: Raven Press. p 19–33.

Karten HJ, Cox K, Mpodozis J. 1997. Two distinct populations of tectal neurons have unique connections within the retinotectorotundal pathway of the pigeon (*Columba livia*). J Comp Neurol 387:449–465.

Laverghetta AV, Shimizu T. 1999. Visual discrimination in the pigeon (*Columba livia*): effects of selective lesions of the nucleus rotundus. Neuroreport 10:981–985.

Laverghetta AV, Shimizu T. 2003. Organization of the ectostriatum based on afferent connections in the zebra finch (*Taeniopygia guttata*). Brain Res 963:101–112.

Lazar G, Toth, P, Csank, G, Kicliter E. 1983. Morphology and location of tectal projection neurons in frogs: a study with HRP and cobalt-filling. J Comp Neurol 215:108–120.

Lin CS, Kaas JH. 1980. Projections from the medial nucleus of the inferior pulvinar complex to the middle temporal area of the visual cortex. Neuroscience 5:2219–2128.

Linke B, De Lima AD, Schwegler H, Pape H-C. 1999. Direct synaptic connections of axons from superior colliculus with identified thalamo-amygdaloid projection neurons in the rat: possible substrates of subcortical visual pathway to the amygdala. J Comp Neurol 403:158–170.

Luksch H, Cox K, Karten HJ. 1998. Bottlebrush dendritic endings and large dendritic fields: motion-detecting neurons in the tectofugal pathway. J Comp Neurol 396:399–414.

Luksch H, Karten HJ, Kleinfeld D, Wessel R. 2001. Chattering and differential signal processing in identified motion-sensitive neurons of parallel visual pathways in the chick tectum. J Neurosci 21:6440–6446.

Major DE, Luksch H, Karten HJ. 2000. Bottlebrush dendritic endings and large dendritic fields: motion-detecting neurons in the mammalian tectum. J Comp Neurol 423:243–260.

Manns M, Güntürkün, O. 1997. Development of the retinotetcal system in the pigeon: a cytoarchitectonic and tracing study with choleratoxin. Anat Embryol 195:539–555.

Marín G, Letelier JC, Henny P, Sentis E, Farfán G, Fredes F, Pohl N, Karten H, Mpodozis J. 2003. Spatial organization of the pigeon tectorotundal pathway: an interdigitating topographic arrangement. J Comp Neurol 458:361–380.

Martinez-Marcos A, Font C, Lanuza E, Martinez-Garcia F. 1998. Ascending projections from the optic tectum in the lizard *Podarcis hispanica*. Vis Neurosci 15:459–475.

Masino T, Grobstein P. 1989. The organization of descending tectofugal pathways underlying orienting in the frog, *Rana pipiens*. I. Lateralization, parcellation, and intermediate spatial representation. Exp Brain Res 75:227–244.

Masino T, Knudsen EI. 1990. Horizontal and vertical components of head movement are controlled by distinct neural circuits in the barn owl. Nature 345:434–437.

Miceli D, Reperant J, Villalobos J, Dionne L. 1987. Extratelencephalic projections of the avian visual Wulst. A quantitative autoradiographic study in the pigeon *Columba livia*. J Hirnforsch 28:45–57.

Mooney RD, Nikoletseas MM, Hess PR, Allen Z, Lewin AC, Rhoades RW. 1988a. The projection from the superficial to the deep layers of the superior colliculus: an intracellular horseradish peroxidase injection study in the hamster. J Neurosci 8:1384–1399.

Mooney RD, Nikoletseas MM, Ruiz SA, Rhoades RW. 1988b. Receptive-field properties and morphological characteristics of the superior collicular neurons that project to the lateral posterior and dorsal lateral geniculate nuclei in the hamster. J Neurophysiol 59:1333–1351.

Nixdorf BE, Bischof HJ. 1982. Afferent connections of the ectostriatum and visual wulst in the zebra finch (*Taeniopygia guttata castanotis* Gould)—an HRP study. Brain Res 248:9–17.

Ogawa T, Takimor T, Takahashi Y. 1985. Projection of morphologically identified superior colliculus neurons to the lateral posterior nucleus in the cat. Vis Res 25:329–337.

Reiner A. 1994. Laminar distribution of the cells of origin of ascending and descending tectofugal pathways in turtles: implications for the evolution of tectal lamination. Brain Behav Evol 43:254–292.

Reiner A, Karten H. 1982. Laminae distribution of the cells of origin of the descending tectofugal pathways in the pigeon (*Columba livia*). J Comp Neurol 204:165–187.

Reiner A, Brecha NC, Karten HJ. 1982a. Basal ganglia pathways to the tectum: the afferent and efferent connections of the lateral spiriform nucleus of pigeon. J Comp Neurol 208:16–36.

Reiner A, Brecha NC, Karten HJ. 1982b. Enkephalin-mediated basal ganglia influences over the optic tectum: immunohistochemistry of the tectum and the lateral spiriform nucleus in pigeon. J Comp Neurol 208:37–53.

Remy M, Güntürkün O. 1991. Retinal afferents to the tectum opticum and the nucleus opticus principalis thalami in the pigeon. J Comp Neurol 305: 57–70.

Roth G, Dicke U, Grunwald W. 1999. Morphology, axonal projection pattern, and response types of tectal neurons in plethodontid salamanders. II: intracellular recording and labeling experiments. J Comp Neurol 404:489–504.

Shepherd IT, Taylor JS. 1995. Early development of efferent projections from the chick tectum. J Comp Neurol 354:501–510.

Shu, SY, Ju G, Fan L. 1988. The glucose oxidase-DAB-nickel method in peroxidase histochemistry of the nervous system. Neurosci Lett 85: 169–171.

Tellegen AJ, Karssen AM, Rietveld TM, Dubbeldam JL. 1998. A crossed projection from the optic tectum to craniocervical premotor areas in the brainstem reticular formation. An anterograde and retrograde tracing study in the mallard (*Anas plathyrhynchos* L.). Eur J Morphol 36:276–243.

Theiss C, Hellmann B, Güntürkün O. 1998. The differential distribution of AMPA-receptor subunits in the tectofugal system of the pigeon. Brain Res 787:114–128.

Uchiyama H, Watanabe M. 1985. Tectal neurons projecting to the isthmo-optic nucleus in the Japanese quail. Neurosci Lett 58:381–385.

Uchiyama H, Yamamoto N, Ito H. 1996. Tectal neurons that participate in centrifugal control of the quail retina: a morphological study by means of retrograde labeling with biocytin. Vis Neurosci 13:1119–1127.

Wang Y, Frost BJ. 1992. Time to collision is signaled by neurons in the nucleus rotundus of pigeons. Nature 356:236–238.

Wang Y, Jiang S, Frost BJ. 1993. Visual processing in pigeon nucleus rotundus: luminance, color, motion, and looming subdivisions. Vis Neurosci 10:21–30.

Wild JM. 1989. Pretectal and tectal projections to the homologue of the dorsal lateral geniculate nucleus in the pigeon: an anterograde and retrograde tracing study with cholera toxin conjugated to horseradish peroxidase. Brain Res 479:130–137.

Woodson W, Reiner A, Anderson K, Karten HJ. 1991. Distribution, laminar location, and morphology of tectal neurons projecting to the isthmo-optic nucleus and nucleus isthmi, pars parvocellularis in the pigeon (*Columba livia*) and chick (*Gallus domesticus*): a retrograde labeling study. J Comp Neurol 305:470–488.

Yamagata M, Sanes JR. 1995. Target-independent diversification and target-specific projection of chemically defined retinal ganglion cell subsets. Development 121:3763–3776.